

METROLOGICAL OPTIMAZITION OF THERMOCOUPLES FOR EXHAUST METERING

Johannes Garbers¹, Stephan Gehrman¹, Silke Augustin², Thomas Fröhlich², Klaus Irrgang³,
Lutz Lippmann³

¹ Porsche AG, Stuttgart, ² TU Ilmenau, Fachgebiet Prozessmesstechnik,

³ Temperaturmesstechnik Geraberg GmbH, Martinroda

ABSTRACT

To improve the measurement of the exhaust gas temperature, the influence of the thermocouple geometry was investigated. Different geometries with a tapered tip and two geometries with a radiation shielding were tested. The numerical calculations and the experimental evaluation showed an improvement in steady state accuracy. The possible improvement in temperature value is 31.6 kelvin comparing the standard and the best working thermocouple geometry. The improvement when comparing the tapered thermocouple to the best working shielded geometry is still 21.4 kelvin. In the experimental evaluation, the time dependent behavior was investigated as well. Here the shielded thermocouple is slightly slower than the tapered thermocouple without shield.

Index Terms – static and dynamic behavior, thermocouple, numerical calculation, application in automobile industry, high temperature, high velocity, Finite Element Method, exhaust system, hot gas test rig

1. INTRODUCTION

Measuring the exhaust temperature with high accuracy is a matter of particular interest for the automotive industry because of the ever increasing demands on the process durability of turbochargers, catalytic converters or particulate filters. It is also important for a better understanding of the combustion process. Harsh ambient conditions occur in exhaust systems, such as high temperatures up to 1000°C, motor vibrations or high pressure values. In addition the process is highly dynamic. These conditions put enormous demands on temperature sensors in use.

The sensor must offer high accuracy, a fast response time, chemical resistance and sufficient thermal-mechanical stability to last inside the exhaust system. Possible sensors for these requirements are resistance thermometers, thermistors or thermocouples. As described in [1] thermocouples are well suited to measure the temperature in exhaust systems. Low thermal mass, which implies lower response time, chemical resistance and thermal-mechanical stability can be achieved with thermocouples.

The static and dynamic characteristics of a thermocouple in exhaust systems were researched both experimentally and numerically in [2]. The authors simulated a thermocouple mounted in a turbocharger housing. Their calculations based on the solution of the Fourier Law of Heat, while calculating the convective heat transfer from the gas using a single heat transfer

coefficient. Their research showed that the heat transfer coefficient has a large influence on the steady state thermal measurement error. However, there are practically no literature references for heat transfer coefficients as well as the other boundary conditions in and around the exhaust system [3]. Therefore it is difficult to determine correct boundary conditions.

2. FUNDAMENTALS

The aim of this paper is to optimize the thermocouple geometry in order to achieve a higher accuracy and a better response time measuring the hot gas temperature. Hence particular importance was placed on the error caused by radiative heat transfer. As shown in [4] and [5] the radiative heat transfer has an influence on the steady state thermal measurement error, especially in high temperature environments.

The radiative heat transfer \dot{Q} emitted by an object is described by the equation

$$\dot{Q} = \varepsilon \sigma A T^4.$$

Usually objects do not emit radiation into free space – they are exchanging radiation with other objects. For example, the radiative heat transfer between two parallel walls can be described with

$$\dot{Q}_{12} = \sigma A E (T_1^4 - T_2^4).$$

The emissivity E between the two walls is given by the equation

$$E = \frac{1}{1/\varepsilon_1 + 1/\varepsilon_2 - 1}.$$

Both equations for \dot{Q} and \dot{Q}_{12} depend on the parameters emissivity ε , surface A and temperature T . One should keep in mind that T signifies the thermodynamic temperature. Because T is raised to the power of four, small temperature differences at high temperature ranges have great influence on the radiative heat transfer.

For the temperature measurement in exhaust systems, the radiative heat transfer mainly occurs between the wall of the exhaust pipe and the thermocouple. The good thermal connection between the exhaust pipe wall and the surroundings causes a lower temperature of the exhaust pipe compared to the thermocouple. Hence, the heat transferred by radiation flows from the thermocouple to the wall. In consequence the thermocouple always has a lower temperature than the gas. An optimization of the gas measurement will occur by raising the temperature of the thermocouple. This can be done by reducing the radiative heat transfer.

As suggested in [4], [5] and also [6] a radiation heat shield is an appropriate measure to reduce the radiative heat transfer. Since the tip of the thermocouple is its hottest point, the protection of the tip is of particular importance. The aim of the research presented here is to develop a radiation shield for the thermocouple tip. A disadvantage of shielding however is a reduction of the convective heat transfer from the gas to the shielded area of the thermocouple. By choosing a suitable shape for the shielding this problem can be reduced. Designs suitable for the use inside exhaust pipes will be investigated.

Different geometries of both thermocouples and shielding were analyzed numerically using FEM modeling. The software package used is Comsol Multiphysics. Convective, conductive and radiative heat transfers are considered in the model. The calculations are performed for steady state conditions.

All thermocouple and shielding geometries modeled numerically were also tested experimentally in a hot-gas test rig.

3. NUMERICAL INVESTIGATION

The unknown boundary conditions mentioned above make a realistic model for the exhaust gas temperature measurement impossible. It is more reasonable to set up an abstract model including all relevant physical effects for the temperature measurement. In this study a part of a pipe was used to represent the exhaust system. A thermocouple was mounted in it. The thermocouple was mounted such that one part of it is located inside the exhaust system and the other part is in contact with the surroundings outside the exhaust pipe. As shown in figure 1 the section of the pipe has a width of 40 mm, the inner diameter is 60 mm and the wall is 1 mm thick. The dimensions of the thermocouple are 110 mm in length and a base diameter of 3 mm.

Certain thermocouples have a tapered tip hence the tip diameter is 1.5 mm. The active tip of the thermocouple is located in the middle of the simulation model; the center of the lower surface of the thermocouple tip is at the point (0, 0, 0) mm. In consequence the section of the thermocouple located inside the pipe is 30 mm long while 79 mm protrude from the pipe. The thermocouple was modeled as homogeneous cylinder. For real thermocouples the welding point of the thermo wires is inside the sheath. A temperature measurement point inside the thermocouple is defined to take the position of the welding point inside the thermocouple into account. The welding point is located normally circa 1 mm deep inside the thermocouple, this means it is 1mm above the lower surface. To take this into account, a measurement point is defined 1 millimeter above the lower surface, its coordinates are (0, 1, 0) mm. The geometry of the simulation model is shown in figure 1.

The materials used for the simulation were air for the exhaust gas, Nimonic Alloy 90 [7] for the thermocouple and steel for the pipe. The material parameters of Nimonic Alloy 90 and steel are assumed to be independent of temperature.

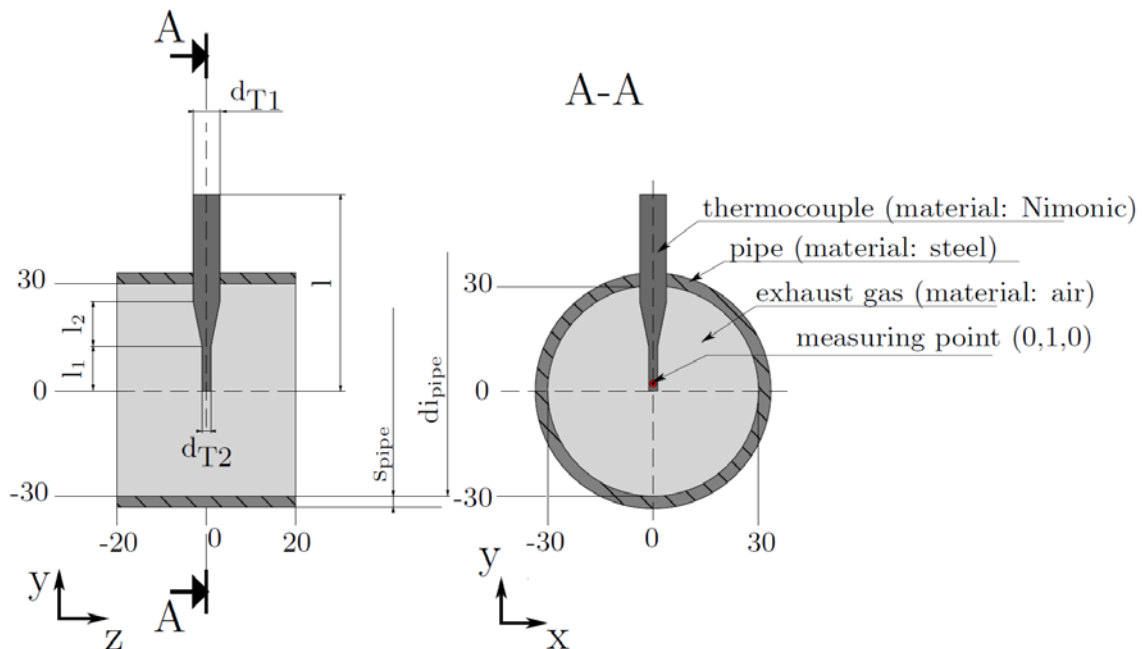


Figure 1- geometry of the model

To take the radiative heat transfer between the pipe, thermocouple and radiative shield surfaces into account, radiative heat transfer is modeled inside the pipe. The interaction with the surroundings outside the pipe is represented by a convective heat transfer coefficient for both the outer wall of the pipe and the outer part of the thermocouple.

In the next step the boundary conditions are applied to the simulation model. Gas flow is assumed to be turbulent and fully developed. Accordingly, the following velocity and temperature distributions are applied at the pipe inlet.

Gas velocity:
$$u_{exh} = 25 \text{ m s}^{-1} + 25 \text{ m s}^{-1} \left(1 - \left(\frac{\sqrt{x^2+y^2}}{R_0} \right)^4 \right)$$

Gas temperature:
$$T_{exh} = 673 \text{ K} + 445 \text{ K} \left(1 - \left(\frac{\sqrt{x^2+y^2}}{R_0} \right)^4 \right)$$

These distributions reach their maximum gas speed and temperature in the center of the pipe. Their values are 50 m s^{-1} for velocity and 845°C for temperature. To describe the convective heat transfer outside the pipe a convective heat transfer coefficient of $\alpha = 12 \text{ W m}^{-2} \text{ K}^{-1}$ and an ambient temperature $T_{ext} = 30^\circ\text{C}$ are assumed. The emissivity used for the radiative heat transfer is $\varepsilon = 0.95$ for all surfaces inside the pipe. Boundary conditions are shown in figure 2.

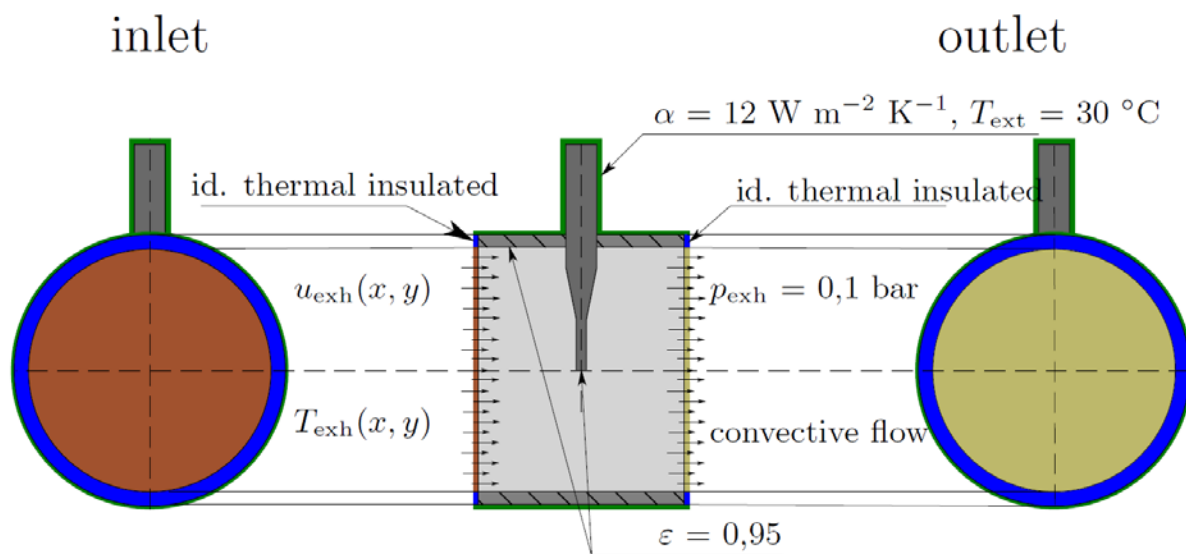


Figure 2 - Boundary conditions for the simulation model

To investigate the influence of different thermocouple shapes four thermocouples were constructed. Geometries 1 and 2 are without a radiation shield while geometries 3 and 4 have a shielding. Every geometry changes only in one parameter, which makes it possible to evaluate the effects of the single parameters. So geometry 1 represents a standard thermocouple and defines the status quo. The next step is a tapered tip, represented by geometry 2. A radiative shielding is added in geometry 3 and in geometry 4 perforations were added to the shielding. The exact description of the geometries is shown in table 1.

The meshing was done with a free tetrahedral mesh, which is shown for geometry 4 in figure 3.


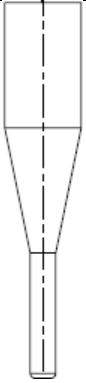
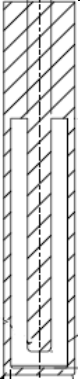
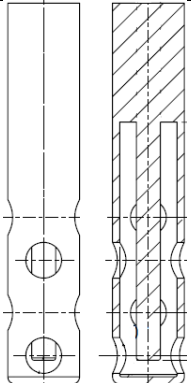
geometry	1	2	3	4
description	standard thermocouple $d_{T1} = 3 \text{ mm}$ $d_{T2} = d_{T1}$	tapered thermocouple $d_{T1} = 3 \text{ mm}$ $d_{T1} = 1,5 \text{ mm}$	like geometry 2, but with not perforated (closed) radiative heat shield	like geometry 2, but with multiple circles perforated radiative heat shield
figure				

Table 1- Presentation of the 4 geometries researched in the study

After the computations the results for the four different thermocouple geometries could be evaluated. At first the flow conditions inside the pipe will be evaluated. For the geometries 1, 2, 3 the gas flow around the cylindrical shape is identical to data from [8], for cylinders in a transverse flow. This leads to a so-called wake space with recirculating flow developing behind the geometries 1, 2 and 3.

For geometry 4 gas flow around the actual thermocouple tip is possible through the perforations in the shield, although some obstruction remains in comparison to the unshielded thermocouples. Viewed from a distance the main effects on the flow are the same as for the other geometries; a global wake space could also be observed behind geometry 4. The gas flow around geometry 4 is more complex. The perforations in the shield produce many small wake spaces and flow disruptions outside and inside of the shield. This is shown in figure 4.

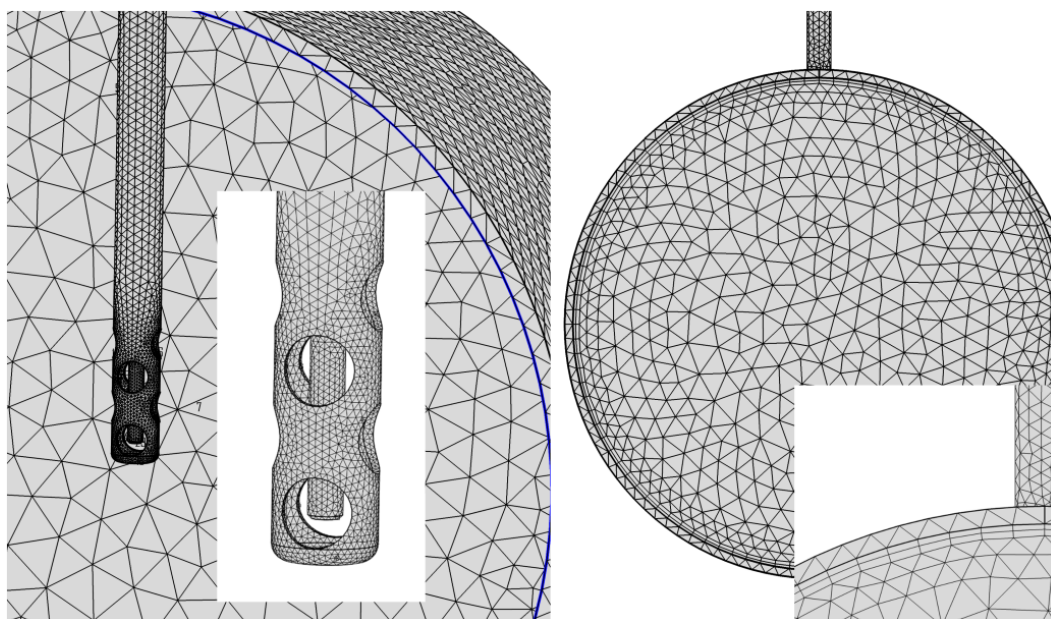


Figure 3 - Meshing shown for geometry 4

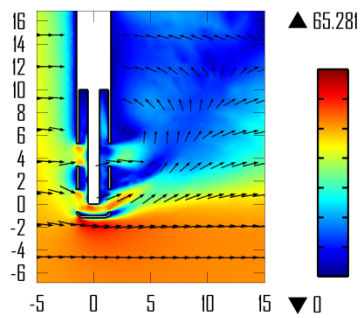


Figure 4 – side view of the fluid flow of geometry 4 [u in ms⁻¹]

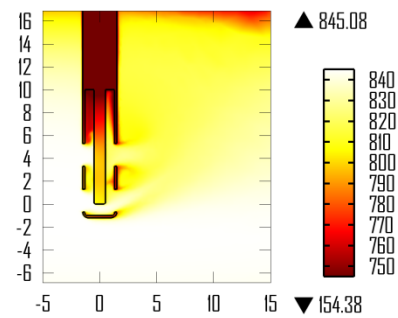


Figure 5 – side view of the temperature field of geometry 4 [T in °C]

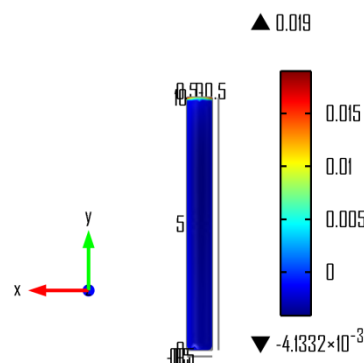


Figure 6 – radiative heat flux, viewed from the inflow direction, geometry 3 [\dot{Q} in W]

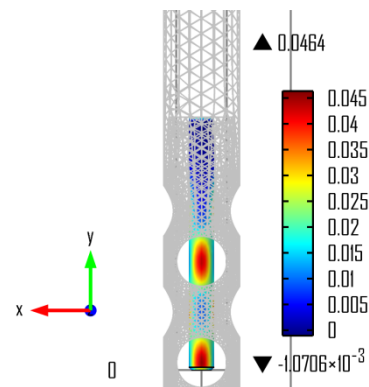


Figure 7 – radiative heat flux, viewed from the inflow direction, geometry 4 [\dot{Q} in W]

For each geometry the overall temperature distributions inside the simulation environment is similar. The hottest exhaust gas is located in the center, around the rotation axes of the exhaust pipe. The tip of the thermocouple is the hottest zone of the body and the temperature of the thermocouple decreases steadily towards the pipe wall. Differences in the temperature distributions are located primarily around the tip of the thermocouple, where the influences of the different shields make themselves felt. The temperature distribution of geometry 4 can be seen in figure 5.

For the simulated area as a whole, inflow and outflow of heat is governed by all the heat transfer mechanisms considered here. Radiation, convection and conduction distribute the inflowing heat energy inside the simulation model and through the outlet boundaries, where the heat leaves the model area again. Outlet heat fluxes occur via the gas flow leaving the pipe section as well as by means of conduction and convection at the solid outer walls. The heat flux inside the simulation environment is influenced only by the different thermocouple geometries.

The main idea of this paper is to minimize the radiative heat loss from the thermocouple in order to reduce the error of the exhaust gas measuring by increasing the temperature of the thermocouple-tip. Hence the evaluation of the simulations is now focused on how the radiation shield influences the heat transfer. The efficacy of the shield can be seen by the amount of radiative heat loss at the tip of the thermocouple. Comparing the heat loss for the thermocouple tips of geometries 3 and 4, it could be shown that the closed protection

geometry is more efficient in protecting the thermocouple-tip from radiative heat loss. The distribution of the radiative heat loss is more homogeneous and also lower compared to geometry 4. This is shown in figures 6 and 7. For geometry 4 there is a higher loss of heat by radiation which is also less evenly distributed along the thermocouple. The inhomogeneity of the radiative heat distribution could be explained by the partial perforation of the shielding geometry. In the areas where the shield is cut out, a high radiative heat flow appears. In the open areas the main radiative heat flow exchange takes place between the wall of the exhaust pipe and the exposed areas of the thermocouple surface. In contrast, the radiative heat exchange of the protected areas of the thermocouple surface happens mainly with the shielding. Since the temperature of the shielding is higher than the wall of the pipe, the absolute temperature difference between the thermocouple and the shielding is lower compared to the absolute temperature difference to the wall of the pipe. The lower temperature difference causes a lower radiative heat loss at the thermocouples surface and this leads to a higher temperature at the tip of the thermocouple.

However, rating the geometries by the temperatures reached at the measurement point, the efficacy for each geometry type must be considered differently. The steady state temperature T_S and the resulting static measurement error for every thermocouple is shown in table 2. Here, the static measurement error ΔT_{th} is defined as the difference between the steady state temperature and the gas temperature (845°C). The lowest measurement error is possible with geometry 4. Comparing geometries 1 and 2 it could also be seen that the smaller diameter of the thermocouple tip for geometry 2 leads to a temperature increase of 13.1 K compared to the temperature of geometry 1. This could be explained by the lower conductive heat flux, caused by the lower tip diameter and also by the increase of the convective heat transfer coefficient for the smaller diameter tip. The influence of the diameter for cylinders in a transverse flow is shown in [4], [8]. Comparing thermocouple geometries 3 and 4 it can be seen that geometry 4 reaches a higher steady state temperature of 801.2 K compared to geometry 3 with 787.9 K. As mentioned above, because of the perforation in geometry 4 the radiative heat loss is higher compared to geometry 3 with a fully closed heat protection. This would lead one to expect geometry 4 to result in a lower measured temperature. This is not the case, however. The explanation could be found in the balance between heat energy input and energy output of the thermocouple. In consequence of the closed heat protection for geometry 3 the exhaust gas could not directly deposit heat into the thermocouple by convective heat transfer. The heat transfer has to occur indirectly by conduction and radiation through the radiative heat protection and also through the enclosed air. In comparison to geometry 4 this causes a lower heat input. If we now take the conductive heat transfer along the TC into account, it becomes apparent that the relative importance of the conductive heat loss through the thermocouple into the surroundings increases as the convective heat input decreases. This results in a lower temperature value at the measurement point for geometry 3.

In case of thermocouple geometry 4 the exhaust gas could flow through the holes in the radiative heat shield. Thus, the heat energy could be transported directly from the exhaust gas to the thermocouple tip by convective heat transfer. This leads to the conclusion that the geometries of the radiation heat protector have to allow a sizeable convective heat inflow from the exhaust gas to the thermocouple tip while at the same time decreasing the loss by radiative heat transport. On the basis of this study it can be expected that a radiation heat

geometry	1	2	3	4
T_S in °C	779.0	792.1	787.9	801.2
ΔT_{th} in K	66.0	52.9	57.1	43.8

Table 2- Measurement point temperatures

protective geometry which makes the best compromise between both heat transport mechanisms can increase the measurement temperature the most.

4. EXPERIMENTAL EVALUATION

To support the results of the numerical simulation, the samples of the thermocouple geometries were investigated experimentally. The investigation was performed in the hot gas test rig at the Temperaturmesstechnik Geraberg GmbH (tmg). In addition to the steady state temperature the dynamic behavior of the thermocouples was also evaluated. A temperature jump between ambient temperature and hot gas temperature was applied to the samples by means of a mechanism which moved the thermocouples rapidly between the inside of the hot gas rig and the surroundings. The tests were performed at a temperature of approx. 1000°C and a flow speed of approx. 50 ms⁻¹. The ambient temperature was estimated to range between 21°C and 35°C. Five jumps from ambient to hot gas and reverse were applied to each sample. The holding time in the hot gas was 3 minutes - long enough to reach steady state temperature for each sample. The mean steady state temperatures T_S are shown in table 3.

From the step response function for the temperature jump the dynamic behavior could be estimated. A workflow described in [4] was executed to estimate the time dependent behavior of the thermocouple samples. In addition to the workflow a second order lag element was used. The calculated time constants for the second order lag element for each thermocouple are shown in table 3. With the calculated time constants the estimated unit-step response could be plotted, as shown in figure 8.

As can be seen in figure 8 and also by the sum time constant τ_Σ in table 3 the thermocouple

geometry	1	2	3	4
T_S in °C	1007.0	1017.2	1010.3	1038.6
τ_1 in s ⁻¹	3.95	1.33	4.25	2.37
τ_2 in s ⁻¹	1.06	0.61	2.21	0.28
τ_Σ in s ⁻¹	5.01	1.94	6.46	2.65

Table 3 - results of the experimental evaluation in the hot gas test rig

geometry 2 shows the shortest time to follow the temperature step, followed by geometries 4, 1 and 3, in this order. Thermal inertia and convective heat transfer are the main influence on the response time of a thermocouple. With both parameters the different response times of the four thermocouples can be explained.

Comparing geometry 2 and 1, both geometries allow undisturbed flow of the exhaust gas around the tip of the thermocouples. So both thermocouples have similar convective heat transfer. But because of the lower diameter of the tip in geometry 2, the thermal inertia mass is lower. So the lower thermal inertia is the main difference between both thermocouples, which causes the difference in the step response. Secondly as mentioned above, along with the lower diameter the convective heat transfer coefficient rises, which also improves the dynamic behavior. Disregarding the additional thermal inertia caused by the mass of the radiative heat shield, geometries 2, 3 and 4 have the same geometric properties, and so the same thermal inertia. That is why the thermal inertia could not explain the difference in the dynamic behavior of the three thermocouple geometries. The explanation could be found in the different flow situations around the tip for every tip of the thermocouples. For geometry 3 no free flow of exhaust gas around the tip is possible. The heat energy has to pass through the

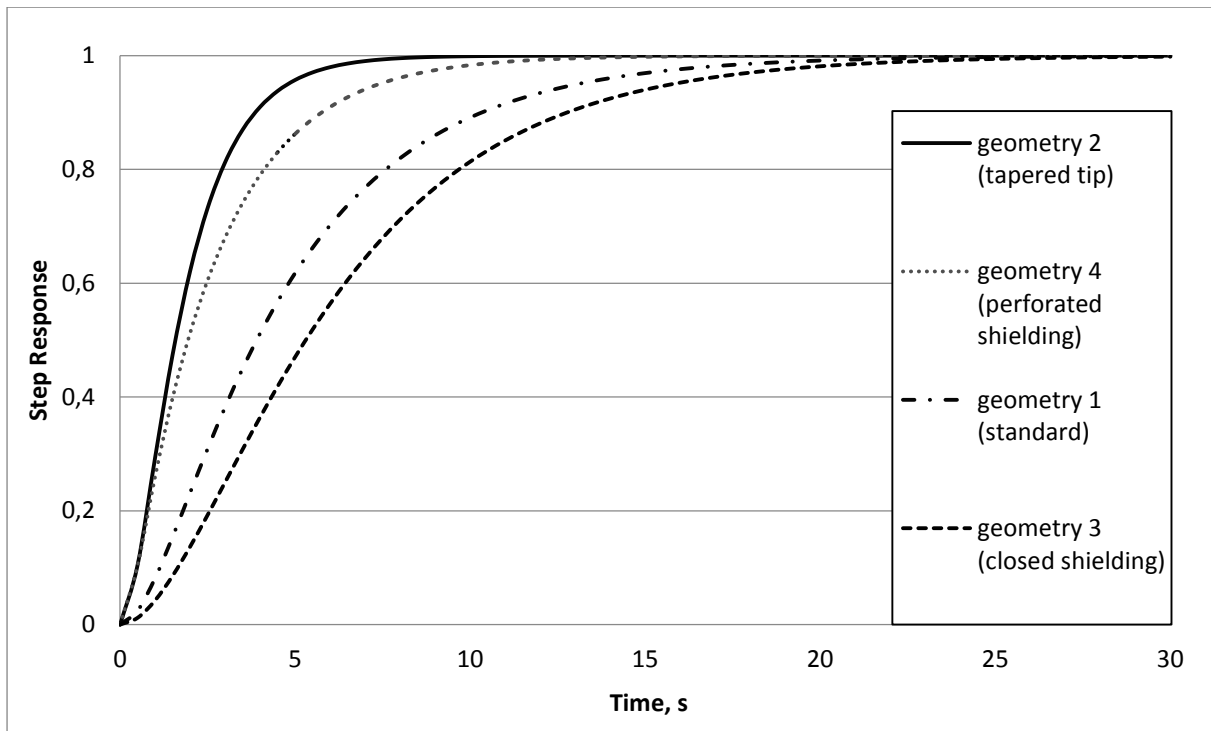


Figure 8 - Unit-Step Response Function for Thermocouple Geometry 1 to 4 (sorted by response time)

wall of the radiative heat shield and also through the volume of air enclosed in the protection geometry. Comparing geometries 2, 3 and 4, the heat flow resistance is largest for geometry 3. Geometry 4 lay between geometry 2 with the best and geometry 3 with the worst heat transfer conditions. That means the flow is hindered by the radiation heat protection, but a direct convective heat transport still is possible. Furthermore comparing geometries 1 and 4 it becomes obvious that the shielding affects the heat transfer so strongly that the thermocouple geometry 1, despite its larger inertia mass, has a better dynamic behavior. In summary the dynamic behavior depends on a small thermal inertia, paired with a good convective heat flow from the gas into the thermocouple.

The results of the hot gas experiment confirmed the numeric calculations for the steady state temperature in general. Unfortunately it was not possible to do the test in the hot gas rig at the same temperature as the simulation. So it is not possible to validate the temperature values directly. Nevertheless the tendency for the different thermocouples could be evaluated.

Geometry 1, without any radiative heat shield, has the lowest steady state temperature with 1017.2°C. Geometry 3 with the best radiative heat protection has a decreased steady state temperature of 1010.3°C. Geometry 4 with the compromise of both discussed heat transfer mechanisms reaches the highest steady state temperature of 1038.6°C. This is an increase of the steady state temperature compared to geometry 2 of 21.4 K. The temperature values reached are shown in table 3.

Comparing the simulation and the experiment the temperatures for the thermocouples show the same tendencies. In both cases geometry 4 reaches the highest temperature value with 801.2°C and 1038.6°C for simulation and experiment respectively. Ranking the thermocouples by the reached temperature at the tip the order for simulation and experiment are the same, shown in table 4.

The experiment in the hot gas rig shows that the thermocouple geometry with a perforated radiative heat shield could increase the steady state temperature, although the time response will be slightly slower.

geometry	simulation	experiment
1	779.0	1007.0
2	792.1	1017.2
3	787.9	1010.3
4	801.2	1038.6

Table 4 - Comparison of the temperature values of the thermocouple for simulation and experiment

5. CONCLUSION AND OUTLOOK

As shown in the previous numerical investigations the geometry of a thermocouple has a strong influence on the measured temperature. A radiative heat shield around the tip of a thermocouple was introduced to increase the measured temperature. Here, the increase of temperature at the measurement point was 9.1 K, compared the thermocouple geometry 2 with tapered tip and geometry 4 with additional radiative heat shielding.

In addition, experimental investigations in a hot gas test rig were performed. Both the steady state temperature and the dynamic behavior were examined. The results show the same effects for steady state temperature as the simulations. For the dynamic behavior, the experiments show that a thermocouple with a tapered tip follows temperature changes more quickly while a radiation heat protector slightly slows down the dynamic reaction.

Depending on the application it should be decided which parameter has priority – steady state temperature or dynamic behavior.

To improve the quality of the numerical results in the future, the test condition in the hot gas test rig should be adapted to the conditions applied in the simulations. In addition more tests in the hot gas test rig should be done to increase the statistical reliability.

The modeling of the thermocouples could be improved by modeling the ceramic powder and the thermo wires inside the sheath. In addition, temperature dependent material parameters should be used. Furthermore in optimization and development of new designs of the radiative heat shield an improvement of static and dynamic behavior could be possible.

Another notable consideration is the thermo-mechanically coupled stability of the thermocouples. In addition for geometry 4 with its inhomogeneous radial arrangement of the perforations in the shield, the influence of the mounting direction has to be investigated. Finally, in a real exhaust system soot from incomplete combustion can be found and could influence the thermocouples. Here the performance of the thermocouples with perforated radiative heat shield is of particular interest.

REFERENCES

- [1] D.P. Culbertson, D.D. Harvey, S.A. Kovaceich, „The Development of Active Thermocouples for Diesel Exhaust Temperature Measurement”, SAE 2008-01-2492, 2008
- [2] S. Augustin, T. Fröhlich, H. Mammen, C. Ament, T. Güther, „Thermoelemente für den Einsatz in Abgassystemen von Verbrennungsmotoren, 2012, Technisches Messen, Oldenburg Wissenschaftsverlag
- [3] S. Augustin, T. Fröhlich, H. Mammen, M. Pufke, „Determination of the dynamic behaviour of high-speed temperature sensors
- [4] Bernhard, Frank (Hrsg.), „Technische Temperaturmessung: Physikalische und meßtechnische Grundlagen, Sensoren und Meßverfahren, Meßfehler und Kalibrierung“, Springer, 2003
- [5] K. Irrgang, M. Lothar, „Temperaturmesspraxis mit Widerstandsthermometern und Thermoelementen.“, Vulkan, 2003
- [6] H. D. Baehr, K. Stephan, “Wärme- und Stoffübertragung”, Springer, 2008
- [7] <http://www.specialmetals.com/documents/Nimonic%20alloy%2090.pdf>, 2013.06.23
- [8] Verein Deutscher Ingenieure; VDI-Gesellschaft Verfahrenstechnik und Chemieingenieurwesen (Hrsg.): „VDI Wärmeatlas: Berechnungsblätter für den Wärmeübergang“, Berlin, Springer-Verlag, 2002

CONTACT

M.Sc. Johannes Garbers

johannes.garbers@porsche.de